Green Chemistry

Hydrogenolysis of cellulose to valuable chemicals over activated carbon supported mono- and bimetallic nickel/tungsten catalysts

Katarína Fabičovicová, Oliver Malter, Martin Lucas and Peter Claus*

The hydrogenolysis of cellulose was systematically investigated at 488 K and under 65 bar H_2 in the absence of a catalyst and over six different catalytic systems containing nickel and/or tungsten on activated carbon (AC) in order to understand the role of individual active components (AC, W/AC, Ni/AC, a physical mixture of Ni/AC + W/AC, and two differently prepared Ni/W/AC catalysts) with respect to the product distribution wherein polyols (*e.g.* ethylene glycol (EG), propylene glycol, and sorbitol) are highly valuable chemicals. Without a catalyst and when using only AC, a hydrochar, due to hydrothermal carbonization of cellulose, was obtained. Although the catalyst W/AC was effective for the degradation of cellulose (high conversion of 90%) and facilitates C−C bond cleavage, selective production of any product was not possible, and the carbon efficiency (CEL) is the lowest (9.1%). Also, with highly dispersed Ni on AC the polyol yield was only 5.3%. The desired behavior showed Ni/W/AC provided its preparation occurs by a two-step incipient wetness (IW) technique. Starting with a remarkably high cellulose/catalyst ratio of 10, a cellulose conversion of 88.4%, CEL of 78.4% and EG yield of 43.7% were achieved (overall polyol yield = 62.1%). Drastically lower yields towards EG by an order of magnitude and decreased CEL were obtained by a co-impregnated Ni/W/AC catalyst and the Ni/AC + W/AC mixture. By the detailed analysis *via* XRD, TPR and CO chemisorption, it can be concluded that in the Ni/W/AC catalyst, after the first IW step of the activated carbon with ammonium metatungstate hydrate and the following reduction in H_2 up to 1128 K, metallic tungsten was formed. This leads, in combination with the hydrogenation properties of nickel introduced in the second IW step, to a virgin bimetallic catalyst, *i.e.* before the hydrogenolysis starts, in which both components must be metallic. This is a prerequisite for high polyol production. Finally, varying the AC type, high space−time-yields up to 2.5 g polyols $(g_{catalyst}\ h)^{-1}$ were obtained. A slight deactivation after two runs followed by a strong decrease of polyol yield in the next two runs was observed. Leaching and structural changes on the catalyst surface (formation of $NiWO_4$) are mainly responsible for deactivation.

1 Introduction

Development of novel chemical processes replacing fossil fuels is one of the main roles of chemistry today.[1] Besides wind-, solar- and hydro-power, which cannot be used for the production of chemicals, the utilization of biomass as feedstock is a sustainable and green method to produce valuable fuels and chemicals.[2] Cellulose constitutes the biggest part of ligno-cellulosic biomass and is the most abundant biopolymer in the world. For this reason and not being in rivalry with food, the degradation of cellulose is the focus of many studies.[3–6]

The early work in 1913 from Bergius[7] showed that it is possible to form bio-coal from cellulose under high temperature. Currently, catalytic conversion of lignocellulosic biomass *via* hydrolysis, solvolysis, hydrothermal liquefaction, pyrolysis or gasification are potential ways to produce valuable fuels and chemicals.[8] As a homogeneous process, liquid acid catalysis is a very effective way to obtain molecules like glucose, xylose or cellobiose from various types of lignocellulosic biomass.[9] Typically, mineral acids like H_2SO_4 or HCl, organic acids such as various carboxylic acids and *p*-toluenesulfonic acid show good performance in liquid acid-catalyzed hydrolysis of cellulose. Nevertheless, these types of cellulose utilization suffer from costly product separation, severe corrosion, and neutralization

*Technical University Darmstadt, Dept. Chemistry, Chemical Technology II,
Alarich-Weiss-Straße 8, 64287 Darmstadt, Germany.
E-mail: claus@ct.chemie.tu-darmstadt.de; Fax: +49 6151 164788;
Tel: +49 6151 165369*

of waste acids. In contrast, heterogeneous catalyst systems have significant advantages (*e.g.* easy separation and recycling of the catalyst after reaction, a non-corrosive procedure and no waste production).[10]

In 2006, Fukuoka and Dhepe[11] reported about the hydrogenolysis of cellulose to sugar alcohols (yield of sorbitol 31%) over supported noble metal catalysts in the aqueous phase and under a hydrogen atmosphere. They used ruthenium and platinum on different support materials, for example SiO_2-Al_2O_3, γ-Al_2O_3 or HUSY. The combination of a metal, which is a hydrogenation component, and a solid acid support which can replace the liquid acid seems to be a very promising green route for cellulose conversion. After this pioneering work, many researchers use various combinations of hydrogenation active sites and acidic solids for the production of commodity chemicals on the basis of cellulose. For example, Ru/C[12] or a combination of Ru/C with heteropoly acids[13] (*e.g.* $H_4SiW_{12}O_{40}$) is very effective for the formation of hexitols (sorbitol and mannitol). If ethylene glycol (EG) is the desired product, catalysts with tungsten species represent a very good choice. For example, a Ni-promoted tungsten carbide catalyst (2%Ni–30% W_2C/AC; AC = activated carbon) catalyses the conversion of cellulose to ethylene glycol with 61% yield at full conversion of cellulose within 30 minutes at 518 K and 60 bar hydrogen pressure (measured at room temperature) with a cellulose/catalyst ratio of 3.3.[14] Furthermore, it was shown that not only the W_2C catalyst but also WO_3, W or H_2WO_4 combined with nickel or noble metals (Ru, Pt, Pd, and Ir) were effective for the production of polyols.[15,16] By optimization of the nickel (or noble metal)/tungsten ratio, high yields of ethylene glycol (>60%) can be achieved. Tai *et al.*[17] assumed that tungsten bronze (H_xWO_3) is the real active component, which is formed during reaction *via* dissolving of tungsten compounds. Cao[18] focused his attention on SBA-15 supported Ni–WO_3 catalysts. A catalyst with a nickel load of 3% and a tungsten trioxide load of 15% had a full conversion of cellulose and a yield of ethylene glycol of 70.7%. The cellulose/catalyst ratio was 4 and the reaction was carried out at 503 K and 60 bar hydrogen pressure measured at room temperature.

In this work, we systematically investigate the behavior of different catalytic systems containing nickel and/or tungsten on activated carbon, which was selected because of the hydrothermal stability, for the hydrogenolysis of cellulose in order to understand the role of individual active components during the conversion of cellulose, and the influence on the obtained product distribution. By a detailed co-analysis of taken liquid samples by HPLC, GC and GC-MS, we were able to quantify 28 various chemical compounds formed during the conversion of microcrystalline cellulose and to follow their complex reaction pathways. We additionally prepared Ni–W catalysts on different kinds of activated carbon and evaluated their performance in the hydrogenolysis of cellulose. The structural features of the catalysts, characterized by means of X-ray diffraction (XRD), temperature-programmed reduction (TPR) and CO chemisorption, were markedly dependent on the preparation method, and had a strong influence on cellulose hydrogenolysis.

2 Experimental

2.1 Catalytical reaction

The experiments were carried out in a stainless steel autoclave (Parr Instrument, 300 mL). Usually, 0.5 g catalyst, 5 g microcrystalline cellulose (Merck) and 100 mL water were stirred (1000 rpm) for 3 hours at a reaction temperature of 488 K and under a hydrogen atmosphere of 65 bar (at reaction temperature). For the reaction the nickel containing catalysts were *in situ* reduced under a hydrogen atmosphere at 753 K. During the reaction, liquid-phase samples were taken and analyzed by HPLC, GC and GC-MS.

2.2 Catalyst preparation

The catalysts used in this work were usually prepared *via* the incipient wetness (IW) method. IW-impregnation of a support material with an aqueous precursor solution and, subsequently, thermal pre-treatment and reduction were performed. In detail, the support material (activated carbon (AC), Norit Rox 0.8 from Cabot Norit Company/Nederland, particle size 0.063–0.2 mm) was first impregnated with aqueous solution of ammonium metatungstate hydrate and then dried at 383 K for 15 h. The dried sample was pretreated under an argon atmosphere at 823 K for 300 minutes. Then, the hydrogen reduction was conducted with a heating ramp: from room temperature to 808 K in 26 minutes and then to 1128 K in 64 minutes. The last step of this procedure was holding this temperature for 30 minutes. After cooling down, the catalyst W/AC was obtained. A second IW-impregnation of the W/AC catalyst with an aqueous solution of nickel nitrate hexahydrate and, subsequently, drying under air conditions at 383 K for 15 h were performed. Subsequently, the catalyst was reduced under hydrogen flow at 713 K for two hours, cooled down and passivated in air/argon flow for 2 hours. The resulting catalyst is Ni/W/AC. The catalyst Ni/AC was prepared only by the second IW-impregnation procedure as described above. The catalyst referred to as Ni/W/AC-coIW was prepared *via* simultaneous co-IW-impregnation of ammonium metatungstate hydrate and nickel nitrate hexahydrate aqueous solution followed by the same treatment as for the W/AC catalyst. Also, the AC type was varied (besides Norit Rox 0.8, also Elorit, MRX, SX Plus, and SX Ultra). Note that the use of different AC particle sizes has been avoided by pestling and sieving each kind of activated carbons in a fraction in the 0.063–0.2 mm range, but the particle size distribution within this range is still unknown.

2.3 Catalyst characterization

2.3.1 XRD. A powder X-ray diffraction (XRD) analysis of the samples was carried out on a StadiP (STOE & Cie. GmbH) diffractometer using $Cu_{K\alpha 1}$-radiation (Ge[111]-monochromator, λ = 1.5406 Å).

2.3.2 TPR. Temperature programmed reduction measurements were done on an apparatus TPD/R/O 1100 (Thermo Fisher Scientific). Therefore the quartz U-tube reactor was loaded with a sample and the catalyst was pretreated in Ar flow

(30 mL min^{-1}) at 383 K for 60 minutes and cooled to 303 K. The H$_2$-TPR was performed using 30 mL min^{-1} of 5.1 vol% H$_2$/Ar by heating the sample from room temperature (303 K) to 1073 K with a heating rate of 5 K min^{-1} while monitoring the TCD signal.

2.3.3 CO chemisorption. Prior to the determination of the dispersion measurements *via* CO pulse chemisorptions, the catalysts were reduced at 623 K for 1 hour followed by cooling down to 273 K in H$_2$ flow. CO chemisorption was performed according to a well-established standard procedure[19] and measured at 273 K by introducing CO pulses with a volume of 0.473 mL into the flowing hydrogen. The latter can be used as a carrier gas because it was shown that pre-adsorption of hydrogen on nickel did not influence the amount of adsorbed CO.[20]

2.4 Experimental evaluation

The conversion X of cellulose was determined gravimetrically based on the weight loss of cellulose during the reaction. In detail, after each experiment, the reaction solution was filtered and the solid residues of cellulose and the catalyst obtained in the folded filter were dried overnight. The difference between the cellulose weight at the beginning of the reaction $m_{Cellulose,start}$, plus the weight of the catalyst m_{Cat} plus the weight of the empty folded filter m_{FF}, and the solid residues inclusive filter $m_{FF,residues}$ yields the amount of utilized cellulose $m_{Cellulose,utilized}$.

$$X\ (\%) = \frac{m_{Cellulose,utilized}}{m_{Cellulose,start}} \times 100$$
$$= \frac{(m_{Cellulose,start} + m_{Cat} + m_{FF}) - m_{FF,residues}}{m_{Cellulose,start}} \times 100 \quad (1)$$

It is important to mention that the determination of cellulose conversion is not valid if any unknown solid products are formed during the reaction. The yields Y_i in this work are based on the moles of carbon in the product i divided by the moles of carbon in cellulose.

$$Y\ (\%) = \frac{c_i}{c_{C_6H_{10}O_5}} \times \frac{n_i}{n_{Cellulose,start}} \times 100 \quad (2)$$

where c_i is the carbon content in the product i; $c_{C_6H_{10}O_5}$ equals 6; $n_{Cellulose,start}$ is the molar amount of cellulose at the beginning of the reaction; and n_i is the molar amount of the product i determined by GC or HPLC. The carbon efficiency CEL was calculated using the ratio of carbon of the known liquid phase products to carbon of all liquid products (known + unknown liquid products).

3 Results and discussion

The heterogeneously catalysed conversion of cellulose to valuable chemicals was under examination in this work. Polyols, *e.g.* ethylene glycol, propylene glycol and sorbitol, were the desired products by a hydrogenolysis process with the heterogeneous Ni–W catalysts described in section 2. However, six

Table 1 CO uptake, Ni dispersion and particle size of different catalysts

#	Catalyst^a	CO uptake (μmol g$_{Cat}^{-1}$)	Ni dispersion (%)	Ni particle size (nm)
1	AC	0.0	—	—
2	W/AC	0.0	—	—
3	Ni/AC	1097.9	64.4	2
4	Ni/AC + W/AC	201.5	(11.8)^b	—
5	Ni/W/AC_coIM	81.9	(4.8)^b	—
6	Ni/W/AC	56.7	(3.3)^b	—

^{a} Tungsten loading = 40 wt% relating to WO$_3$. Nickel loading = 10 wt%. ^{b} See text.

different materials (Table 1), including also monometallic catalysts, were prepared to understand the role of individual catalyst components for cellulose hydrogenolysis/hydrogenation. Thus, the performance of the Ni/W/AC catalyst prepared by the described two-step IW impregnation technique was compared to the following catalysts: AC, W/AC, Ni/AC, a physical mixture of Ni/AC + W/AC, and the co-impregnated catalyst Ni/W/AC_coIW. The experiments showed remarkable differences in product spectra and conversion of cellulose (Table 2). The reaction without a solid catalyst was also examined.

3.1 Reaction without a catalyst

Under hydrothermal conditions a hydrochar, a muddy black solid product, was obtained due to hydrothermal carbonization (HC). As mentioned above, if unknown solid products were formed during the reaction, determination of cellulose conversion by eqn (1) is incorrect because the obtained solid products are included in the folded filter. Visual tests showed that no white leftover of cellulose could be found in the solid residues. Because of this, it was assumed that full conversion of cellulose in the experiment without a catalyst was achieved.

A change in chemical structure of the hydrochar obtained by the HC reaction of cellulose in comparison with raw cellulose was examined by an analytical method based on diffuse reflectance coupled with infrared Fourier transform spectroscopy (DRIFTS, Bruker Equinox 55 IR spectrometer). Bands typical for cellulosic material and its carbonaceous degradation products were found in our samples (Fig. 1). The hydrochar spectra consist of several bands: a wide band at 3650–3000 cm^{-1} shows the presence of O–H stretching vibrations in hydroxyl or carboxyl groups.[21] Bands in the 1300–1000 cm^{-1} region present C–O stretching vibrations, characteristic for hydroxyl, phenol or ether and also for O–H bending vibrations.[22,23] The presence of other oxygen groups is suggested by the band at 1710 cm^{-1}, which corresponds to C=O vibrations of carbonyl, quinone, ester or carboxyl[24] groups. In the region 1450–1380 cm^{-1}, C–H deformations (symmetric or asymmetric) can be found.[22] A band typical for the aromatic skeletal is at 1510 cm^{-1}.[22] The signal at 1610 cm^{-1} belongs to C=C vibrations of aromatic rings.[25] Chemical structure differences are evident in DRIFTS traces between raw cellulose and hydrochar. A significant increase (in comparison to raw cellulose) of the intensity of the bands

Table 2 Cellulose conversion and product yields for different catalysts by a reaction temperature of 488 K and a hydrogen pressure of 65 bar (measured at reaction temperature) for 3 hours

#		Without catalyst	AC	W/AC	Ni/AC	Ni/AC + W/AC	Ni/W/AC_coIW	Ni/W/AC	
X/%		70.5[a]	76.4[a]	90.4	71.7	93.7	85.3	88.4	
CEL/%		16.8	29.9	9.1	41.1	27.1	34.1	78.4	
Yield/%	MeOH	0.0	0.0	0.0	<0.1	0.1	0.1	0.7	C1
	EtOH	0.0	0.0	0.0	<0.1	0.1	0.2	0.47	C2
	EG	<0.1	<0.1	<0.1	2.0	4.3	5.6	43.7	
	AA	2.0	2.4	3.0	0.3	1.1	0.4	<0.1	
	PG	0.0	0.0	0.0	0.6	1.2	1.4	5.0	C3
	G	0.0	0.0	<0.1	<0.1	0.2	0.3	0.4	
	HA	0.9	2.1	0.9	9.1	5.3	6.3	1.8	
	Ac	0.3	0.3	0.3	<0.1	<0.1	0.0	0.0	
	BDO	0.0	0.0	0.0	<0.1	0.2	0.4	4.0	C4
	Erythritol	0.0	0.0	0.0	0.3	0.5	0.7	2.4	
	1-OH-2-B	0.4	0.4	0.8	7.3	4.6	7.1	1.4	
	Acetoine	0.6	0.7	1.1	1.5	3.9	1.8	0.3	
	LA	1.0	4.4	0.8	0.0	0.0	0.0	0.0	C5
	Furfural	1.1	1.9	0.1	0.4	0.0	0.0	0.0	
	Xylitol	1.9	2.1	0.0	1.0	0.0	<0.1	<0.1	
	Sorbitol	0.3	0.0	0.2	0.9	1.3	5.9	5.9	C6
	AcA	0.5	0.8	0.7	2.6	2.3	0.8	0.8	
	HMF	1.1	6.0	0.0	0.6	0.0	0.0	0.0	
	Sugars	1.9	2.0	0.3	2.3	0.0	1.3	0.5	

MeOH – methanol, EtOH – ethanol, EG – ethylene glycol, AA – acetic acid, PG – propylene glycol, G – glycerol, HA – hydroxy acetone, Ac – acetone, BDO – butanediol, 1-OH-2B – 1-hydroxy-2-butanone, acetoine – 3-hydroxy-2-butanone, LA – levulinic acid, AcA – acetonyl acetone, HMF – 5-hydroxymethylfurfural, sugars – cellobiose, glucose, mannose, fructose. [a] Hydrochar particles were obtained. Gravimetrically calculated conversion is not valid. Conversion can be assumed to 100% (see text).
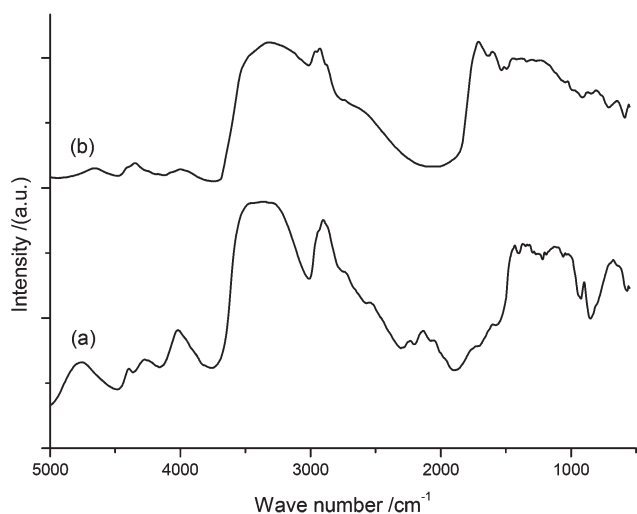
Fig. 1 DRIFT spectra of raw cellulose (a) and hydrochar produced by the reaction of cellulose without a catalyst (b).

at 1510 cm^{-1} and 1610 cm^{-1} suggests that more aromatic structures are present in the hydrochar. Also the strong increase of the band at 1710 cm^{-1} which is typical for carbonyl, quinine, ester or carboxyl C═O vibrations confirms that the cellulose was strongly changed. Sevilla *et al.*[26] reported about dehydration during the HC reaction of cellulose, which was identified by a decrease (in relation to raw cellulose) of intensity of the bands at 1460–1000 cm^{-1} and 3700–3000 cm^{-1}. These results were also confirmed during the measurements of our samples.

Aldehydes, ketones, and organic acids (*e.g.* hydroxy acetone, 1-hydroxy-2-butanone, 3-hydroxy-2-butanone (acetoine), or acetic acid) were detected in the liquid phase (Table 2). C6 and C5 compounds like levulinic acid, furfural, xylitol, HMF or glucose were the predominant products. The received product distribution, the low summarized yield of known products in the liquid phase (11.8%) and also the low carbon efficiency (16.8%) prove true the mechanism of hydrothermal carbonization of cellulose giving rise to the formation of hydrochar, which is a well-studied process.[26,27] The latter includes several steps (*e.g.*, cellulose hydrolysis, glucose isomerisation to fructose, dehydration, aldol condensation, agglomeration/growth of particles producing hydrochar)[26] explaining the observed products.

3.2 Activated carbon

Very similar products to those obtained in experiments without a catalyst were also found in experiments using only AC (Table 2). However, the amount of identified known soluble compounds was higher in comparison with the HC reaction with a summarized yield of ~23%. Especially, HMF, furfural and levulinic acid were produced with yields of 6%, 1.8% and 4.4%, respectively. These degradation products of cellulose are valuable chemicals and are typically formed in halide-catalyzed processes.[28–38] For the reactions over AC or sulfonated AC, usually glucose is a degradation product[39,40] which was produced in our case with minor yield (1.8%). However, hydrochar was also formed in the reaction with AC and an unknown amount of carbon atoms ends up in undesired solid products. Consequently, similar to the HC reaction, the value of the

carbon efficiency coefficient was low, 29.9%. Short-chain polyols like propylene glycol or butanediol were not detectable and the yield of ethylene glycol was <0.1%.

3.3   W/AC

This catalyst showed a high cellulose conversion of nearly 90% (W/AC, Table 2). Although this high value was achieved, the carbon efficiency coefficient was only 9.1%. Note that the amount of unknown soluble products was higher compared to other experiments. Non-identified gray/black oily solid products were also obtained during this reaction, which shows that an unknown amount of carbon can be found in the solid phase. It is important to mention that, based on a visual test, the solid product was different compared to the hydrochar obtained during the HC reaction of cellulose without a catalyst and with AC. Due to the high activity of W/AC, the formation of gas phase products is also possible and, indeed, methane and carbon dioxide were formed during the reaction. It is interesting to note that in the case of W/AC the yield of typical acid-catalyzed degradation products of cellulose (HMF, furfural, levulinic acid) is considerably lower compared to AC (see Table 2). The amount of C6 and C5 compounds formed over W/AC was drastically smaller (2.1%) than with AC (17%) or without the catalyst (7.6%) and short-chain compounds like acetic acid were predominant. Consequently, the catalyst containing tungsten is effective for the degradation of cellulose in order to achieve high cellulose conversion and facilitates C–C bond cleavage, but a highly selective production of any product is not possible.

3.4   Ni/AC

If nickel on activated carbon was used as a catalyst, a new product distribution was achieved (Table 2). The active sites of nickel catalysts are well-known for their hydrogenation properties[30] and during the conversion of cellulose many different reaction pathways are possible. Short-chain compounds like ethylene glycol, propylene glycol, butanediol, or glycerol were formed. Also, other polyols like sorbitol, erythritol, 1,2-hexanediol, or 1,2,6-hexanetriol were built up in reactions with Ni/AC. Interestingly, ketones like hydroxy acetone, 1-hydroxy-2-butanone, acetonyl acetone, and acetoine were identified with yields of 9.1%, 7.3%, 2.6% and 1.5%, respectively. The experiment with Ni/AC opened reaction pathways towards the production of polyols, but their yield is rather low (5.3%). In the next step, catalysts which compromise nickel and tungsten in one catalytic system were studied.

3.5   Ni/AC + W/AC, Ni/W/AC_coIW, Ni/W/AC

Conversions of cellulose and the yields of produced components for our experiments with catalysts containing nickel and tungsten on activated carbon are listed in Table 2. To prove the synergetic effect of nickel and tungsten and the influence of structure of these catalysts on the catalytic properties, we tested three different systems: a physical mixture of Ni/AC and W/AC (Ni/AC + W/AC), the co-impregnated Ni/W/AC_coIW and the Ni/W/AC catalyst prepared with the two-step

impregnation procedure. The amounts of formed compounds differed strongly. Interestingly, notable yields of ketones occurred over the mixture of Ni/AC + W/AC and over Ni/W/AC_coIW, which was similar to the experiment with Ni/AC. Hydroxy acetone, 1-hydroxy-2-butanone, acetonyl acetone, and acetoine were observed with a summarized yield of 20.5% for Ni/AC, 16.1% for Ni/AC + W/AC and 16.6% for Ni/W/AC-coIW. Surprisingly, the yield of these compounds for the catalyst Ni/W/AC was only 4.3%. As expected, the amount of polyols was also changed in these investigated catalyst systems. For the reaction with the mixture of Ni/AC and W/AC and the Ni/W/AC_coIM catalyst, the yield of polyols was only 7.9% and 10.3%, respectively. This is different from the literature,[41] where it was claimed that for high EG yields the two functional components for cellulose degradation and hydrogenation can be combined by simple co-reduction or by simple physical mixing. The desired behavior in order to produce ethylene glycol with a very high yield showed the catalyst Ni/W/AC. Starting with a high cellulose/catalyst ratio of 10, a cellulose conversion of 88.4% and a yield of ethylene glycol of 43.7% were achieved. The summarized yield of all obtained polyols is equal to 62.1%. This corresponds to a space–time-yield of 1.6 g ethylene glycol $(g_{catalyst}\ h)^{-1}$ and 2.2 g polyols $(g_{catalyst}\ h)^{-1}$. Note that the quantity of ketones was drastically smaller compared to the co-impregnated catalyst and the mixed catalyst.

3.6   Structural features of the catalysts

The XRD patterns of the catalysts are shown in Fig. 2. Keeping in mind that, after IW impregnation of the activated carbon with ammonium metatungstate hydrate and the following drying steps (see section 2.2), this material was reduced in H_2 up to 1128 K, the formation of metallic tungsten can be expected, which is typically formed in the temperature range 1023–1273 K.[42]

For the catalyst Ni/AC (Fig. 2, curve (a)) no peak for nickel could be found. The catalyst Ni/W/AC (Fig. 2, curve (c)) showed a very small peak corresponding to nickel at 2Theta = 44.2°.
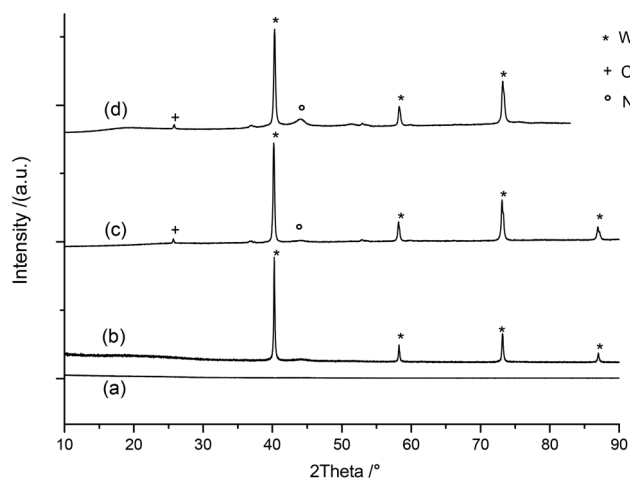

Fig. 2   XRD patterns of various catalysts: (a) Ni/AC, (b) W/AC, (c) Ni/W/AC, (d) *in situ* reduced Ni/W/AC.

This can be caused by a passivation of nickel catalysts after the preparation procedure. Because of the passivation, we reduced the catalyst Ni/W/AC *in situ* before the XRD pattern was measured (Fig. 2, curve (d)). After the *in situ* reduction, peaks corresponding to metallic nickel species (at 2Theta = 44.2°, 51.5°, and 75.7°) were obtained with a higher intensity. The comparison of the passivated and *in situ* reduced Ni/W/AC catalyst is much more clearly illustrated in Fig. 3. If the catalyst was prepared *via* the co-IW method (Ni/W/AC_coIW), then W_2C, Ni_2W_4C and WO_3 were detected, but the peaks were very small (not shown in this paper).

TPR curves (Fig. 4) of various catalysts give more information about H_2 consumption, reducibility of the catalyst surface and also about metal–metal interaction. For the AC support (Fig. 4, curve (a)) a broad peak with low intensity around 900 K was observed. By coupling TPR with a mass spectrometer, CH_3 and CH_4 signals were detected, which

clearly indicates the methanation of this material. The W/AC catalyst showed a very similar TPR profile (Fig. 4, curve (b)) in comparison with AC, suggesting no existence of reducible tungsten species. However, as mentioned above this is caused by the use of a high reduction temperature (1128 K) during the preparation procedure for tungsten pre-catalyst reduction. This also corresponds with XRD results showing only the presence of irreducible metallic W in the W/AC catalyst. For the catalysts containing nickel, there are more sets of peaks in TPR profiles, one in the region of 400–500 K, and another broad peak around 750 K. Because of the passivation procedure after the catalyst preparation, NiO was formed. The observed reduction peak in the range of 400–500 K could be allocated to NiO reduction, which is typical for Ni catalysts. The second reduction peak belongs to the methanation of the AC support, which was confirmed by the presence of CH_3 and CH_4 signals in the mass spectrometer (Fig. 5). As expected, the Ni/AC catalyst and a physical mixture of Ni/AC + W/AC gave related profiles (Fig. 4, curves (c) and (d)). Therein, no interaction was found between tungsten and nickel. The catalyst Ni/W/AC (Fig. 4, curve (f)) showed lower hydrogen consumption for the first reduction peak at 400–500 K, in contrast to Ni/AC, where the hydrogen consumption for this peak was very high (comprises more NiO). It can be disclosed that the catalyst obtained after the two-step IW impregnation must contain two active constituent parts: metallic tungsten for the degradation of cellulose and nickel for the subsequent hydrogenation step. Both components must be metallic in the virgin bimetallic catalyst,
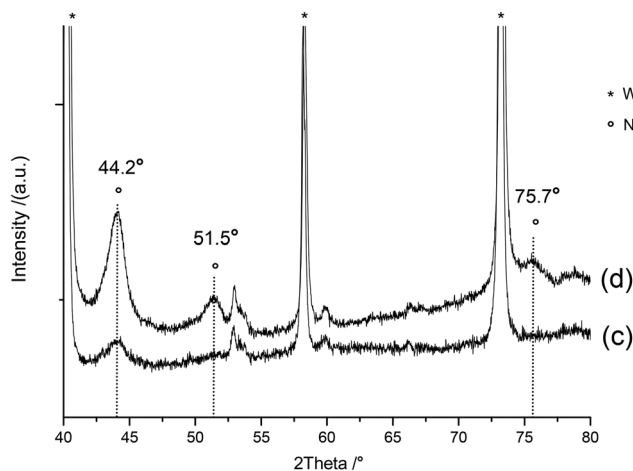

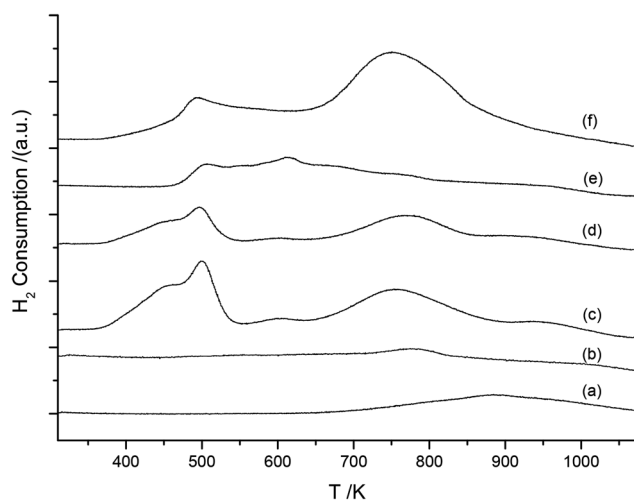**Fig. 3** Enlarged detail of the XRD patterns of (c) Ni/W/AC and (d) *in situ* reduced Ni/W/AC.

Fig. 4 H_2-TPR patterns of various catalysts: (a) AC, (b) W/AC, (c) Ni/AC, (d) Ni/AC + W/AC, (e) Ni/W/AC_coIW, (f) Ni/W/AC.
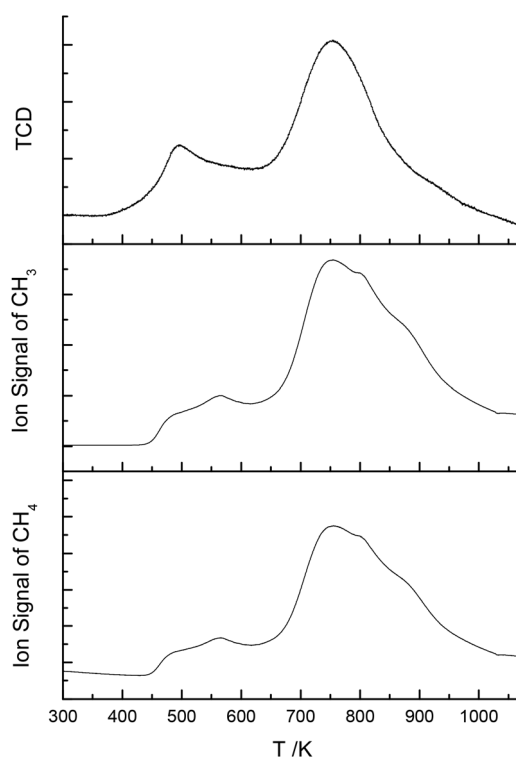

Fig. 5 TCD signal of hydrogen consumption and ion signals for CH_3 and CH_4 during the TPR of Ni/W/AC catalyst.

Table 3 Texture data of active carbon supported Ni/W catalysts and space–time-yields of ethylene glycol and polyols in cellulose hydrogenolysis

| Catalyst	Specific surface area of AC[a]/m^2 g^{-1}	Dubinin surface area of prepared catalyst[b]/m^2 g^{-1}	Micropore content/%	Space–time-yield of EG/g$_{EG}$ (g$_{Cat}$ h)$^{-1}$	Space–time-yield of polyols/g$_{Polyols}$ (g$_{Cat}$ h)$^{-1}$
Ni/W/AC-Elorit	700	434	69	1.1	1.7
Ni/W/AC-MRX	850	565	62	1.6	2.1
Ni/W/AC-SX Plus	1100	604	68	1.9	2.5
Ni/W/AC-SX Ultra	1200	645	66	1.8	2.5
Ni/W/AC-Norit Rox 0.8	1225	651	82	1.6	2.2

[a] Manufactured information. [b] Measurements on Sorptomatic 1990.

i.e. before hydrogenolysis starts, which is a prerequisite for high polyol production. Indeed, it is confirmed by the high yield of polyols (62%) during reaction with the Ni/W/AC. That the catalyst preparation method has a significant effect on reduction properties and performance of a catalyst is well-known. This influence can be seen in the TPR pattern of the co-impregnated catalyst Ni/W/AC_coIW (Fig. 4, curve (e)). In comparison with the Ni/W/AC catalyst prepared *via* the two-step IW procedure, a different reduction behavior was achieved. A peak with a plateau was observed in the range from 500 K to 600 K and the hydrogen consumption was significantly lower in comparison with the Ni/W/AC catalyst. With reference to the XRD analysis of the Ni/W/AC_coIW catalyst, where Ni$_2$W$_4$C (besides WO$_3$) was found, it can be concluded that the different reduction behavior is due to the simultaneous impregnation of the active carbon with the Ni and W precursors, leading to the above mentioned nickel–tungsten phase. If the latter is present in the catalyst the yield of ethylene glycol and the carbon efficiency are much lower (Table 2).

Chemisorption of CO conducted at 273 K with the catalysts investigated in this work (Table 1) was very different. No CO adsorption took place on the catalysts W/AC and AC. This corresponds with the experimental results that no or very small amounts of hydrogenated compounds were formed during the reactions over these catalysts. The Ni/AC catalyst adsorbed a high amount of CO molecules (1097.7 µmol g$_{Cat}$$^{-1}$). The calculated dispersion of nickel was 64%, and from that, the average nickel particle size can be calculated, which is very small (2 nm). For catalysts containing tungsten, a significant decrease in CO adsorption was obtained. The calculated dispersions are not representative in these cases (values in brackets in Table 1) because of possible interactions between tungsten and nickel species (*e.g.* coverage of particles).

3.7 Influence of the AC support

Consequently, the most effective catalyst for ethylene glycol production from cellulose was the Ni/W/AC catalyst prepared *via* the two-step IW-impregnation. However, not only nickel and tungsten have a significant influence on selective production of ethylene glycol and other polyols. The kind of support material is also important and can improve the formation of desired compounds. To see this influence, nickel/tungsten catalysts on different activated carbons were prepared and tested (Table 3, Fig. 6). Note that ethylene glycol is the
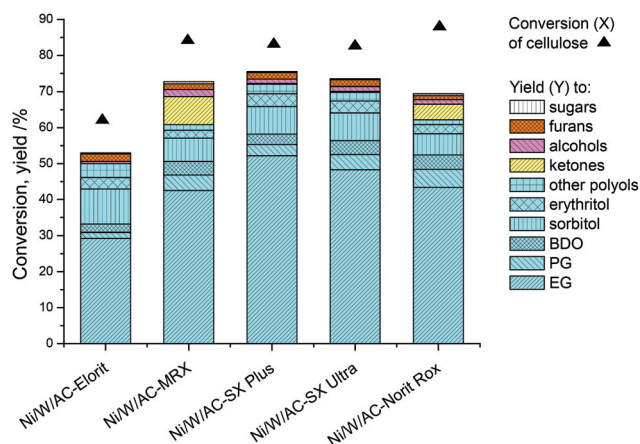
Fig. 6 Conversions of cellulose and yields for Ni/W catalysts on different activated carbons. Reaction conditions: 488 K, 65 bar H$_2$ (at reaction temperature), 5 g cellulose, 0.5 g catalyst, 100 mL deionised water, 1000 rpm, 3 hours.

main product with high yield (> 40%) for catalysts exhibiting surface areas >500 m^2 g^{-1}, independent of the AC type used, with the exception of Ni/W/Elorit (EG yield: 29.3%). With increasing surface area the conversion of cellulose was increased (Fig. 6). However, the differences in activity/space–time-yield may be not only the result of their specific surface areas, but are also due to different production technologies of the activated carbons (*e.g.*, Elorit and MRX: the steam activation process; SX Plus, SX Ultra and Norit Rox 0.8: the steam activation process and acid washing), and their surface properties. It is well-known that activated carbon in the presence of water exhibits acidic character because of the functional groups (COOH, phenolic, anhydride, *etc.*),[43] however, it is beyond the aim of the present study to characterize the latter in detail, for example by IR spectroscopy. The obtained space–time-yield is the highest for Ni/W/AC SX Plus (1.9 g ethylene glycol (g$_{catalyst}$ h)$^{-1}$ and 2.5 g polyols (g$_{catalyst}$ h)$^{-1}$).

3.8 Recycling/active species

For heterogeneous catalysts, stability is one of the most important challenges. Therein, we conducted a recycling test with the Ni/W/AC-SX Ultra catalyst. The recycling test was carried out in an autoclave with 1 g catalyst, 5 g cellulose and 100 mL deionized water under a reaction temperature of 498 K and a

65 bar hydrogen atmosphere. For the re-use, it is necessary to recover the catalyst without residues of cellulose. Therefore, in the recycling test, the reaction temperature of 498 K was employed because of full conversion of cellulose which is achieved at this reaction temperature within 3 hours. At the reaction temperature of 488 K, the cellulose conversion was 88.4%. In Fig. 7, it is obvious that the yield of polyols slightly decreased from 77.8% to 63.4% in the second run. Then, in the third run, a significant decrease in polyol yield to 2.4% was obtained. After the third run, we reduced the recovered catalyst *in situ* under hydrogen flow followed by the fourth recycling run. The second reduction cannot renew the activity of the catalyst, and the yield of polyols was only 0.3%. Note that along with the almost complete absence of polyols, an increase of production of ketones was noticeable. Interestingly, the ICP analysis of the liquid products shows that after the first run the concentrations of nickel and tungsten in the liquid phase were 0.05 g L^{-1} and 0.137 g L^{-1}, respectively. After the second recycling run, concentrations of 0.05 g L^{-1} of nickel and 0.058 g L^{-1} of tungsten were found. The losses of Ni and W in the third repeated cycle were 0.037 g L^{-1} and 0.022 g L^{-1}, respectively, and in the last run, nearly the same (0.036 g L^{-1} for nickel and 0.020 g L^{-1} for tungsten). We can conclude that the deactivation of the Ni/W/AC catalyst is connected with an overall loss of weight of 17.2% for nickel and 7.8% for tungsten during the four recycling tests. Despite the maximum nickel and tungsten leaching after the first run of our experiments the only slight decrease of polyol and EG yield indicates that the Ni/W ratio may be still intact until further leaching of both components during the following re-use experiments changes both the activity and the product distribution. Now mainly ketones were formed (see Fig. 7) due to the decreased nickel concentration on the catalyst surface and, thus, the partial loss of the hydrogenation function. We already observed this mechanism of deactivation in the glucose hydrogenation to sorbitol.[44] Note that reaction products of cellulose

hydrogenolysis (glucopyranosides, polyols) have metal-binding sites[45] acting as chelating components. Therefore, although in the course of the 1st run, polyol formation is increased on the one hand, this caused leaching and the deactivation process proceeds more and more in the re-use experiments on the other hand. Moreover, polyols like EG play also a role in the formation of nickel tungstate, $NiWO_4$,[46] which was detected by XRD measurement after the reaction. The formation of that kind of tungsten bronze[47] under the hydrothermal conditions of our experiments implies the presence of nickel ions (due to leaching) and tungsten oxidation (to WO_3 layers onto W) which depends on temperature and the ratio of the partial pressures of H_2O/H_2. For the latter process the reaction rate is approximately equal to 1.6 g_W m^{-2} h^{-1} at elevated temperature and pressure (423–633 K, 70–80 bar[47]) similar to the reaction conditions of our work. Following the recently published results, tungsten species in a broad range of valence states (0 to +6) are effective in degradation of cellulose.[16,17,41,48] Similar to our observation of surface $NiWO_4$, the work of T. Zhang *et al.* revealed that the interplay of tungstenic acid (H_2WO_4) and soluble hydrogen tungsten bronze (H_xWO_3) is important in cellulose hydrogenolysis,[17,41] the latter being the active species.

In conclusion, we investigated six catalytic systems for cellulose hydrogenolysis (and the reaction without catalyst) in order to obtain more information about the role of individual active components with respect to the formation of valuable products from cellulose such as polyols, *e.g.* ethylene glycol. We could confirm that tungsten species are very effective for cellulose degradation in order to achieve very high conversion; however, polyol production with the monometallic catalyst W/AC is low and requires combination with the hydrogenation properties of nickel. Based on our results, the catalyst obtained after the two-step IW impregnation must contain two active constituent parts: metallic tungsten for the degradation of cellulose and nickel for the subsequent hydrogenation step. Our investigation clearly revealed that both components must be metallic in the virgin bimetallic catalyst, *i.e.* before hydrogenolysis starts. Catalysts in which the two functional components for cellulose degradation and hydrogenation were combined by simple co-reduction or by simple physical mixing did not produce ethylene glycol, and the EG yield is one order of magnitude lower. Under the hydrothermal conditions of hydrogenolysis, in the presence of H_2 and reaction products (*e.g.* polyols), structural changes of the catalyst surface are possible. Unfortunately, they cannot be monitored by *in situ* characterization methods which are actually not available in the case of such kinds of gas/liquid/solid–solid reaction systems.
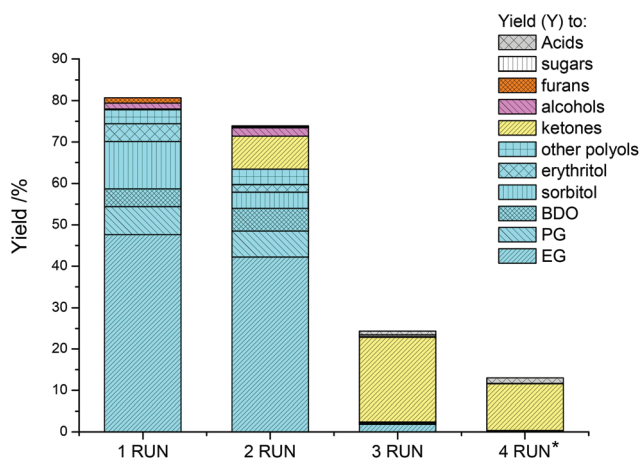

Fig. 7 Yields for Ni/W/AX-SX Ultra catalyst in the recycling test. Reaction conditions in each run: 498 K, 65 bar H_2 (at reaction temperature), 5 g cellulose, 1 g catalyst, 100 mL deionised water, 1000 rpm, 3 hours, *catalyst 2nd time reduced.

Acknowledgements

References

1 P. Gallezot, *Catal. Today*, 2007, **121**, 76–91.

2 R. Palkovits, *Chem. Ing. Tech.*, 2011, **83**, 411–419.

3 R. Palkovits, K. Tajvidi, J. Procelewska, R. Rinaldi and A. Ruppert, *Green Chem.*, 2010, **12**, 972–978.

4 R. Rinaldi, R. Palkovits and F. Schüth, *Angew. Chem., Int. Ed.*, 2008, 47, 8047–8050.

5 P. Dhepe and A. Fukuoka, *Catal. Surv. Asia*, 2007, **11**, 186–191.

6 S. Van de Vyver, L. Peng, J. Geboers, H. Schepers, F. de Clippel, C. J. Gommes, B. Goderis, P. A. Jacobs and B. F. Sels, *Green Chem.*, 2010, **12**, 1560–1563.

7 F. Bergius, *J. Soc. Chem. Ind.*, 1913, **32**, 462–467.

8 C. H. Zhou, X. Xia, C. X. Lin, D. S. Tong and J. Beltramini, *Chem. Soc. Rev.*, 2011, **40**, 5588–5617.

9 R. Rinaldi and F. Schüth, *ChemSusChem*, 2009, **2**, 1096–1107.

10 R. A. Sheldon and H. van Bekkum, in *Fine Chemicals through Heterogeneous Catalysis*, Wiley-VCH Verlag GmbH & Co. KGaA, Weinheim, 2007, pp. 1–11.

11 A. Fukuoka and P. L. Dhepe, *Angew. Chem., Int. Ed.*, 2006, **45**, 5161–5163.

12 C. Luo, S. Wang and H. Liu, *Angew. Chem., Int. Ed.*, 2007, **119**, 7780–7783.

13 R. Palkovits, K. Tajvidi, A. M. Ruppert and J. Procelewska, *Chem. Commun.*, 2011, **47**, 576–578.

14 N. Ji, T. Zhang, M. Zheng, A. Wang, H. Wang, X. Wang and J. G. Chen, *Angew. Chem., Int. Ed.*, 2008, **120**, 8638–8641.

15 Y. Zhang, A. Wang and T. Zhang, *Chem. Commun.*, 2010, **46**, 862–864.

16 M.-Y. Zheng, A.-Q. Wang, N. Ji, J.-F. Pang, X.-D. Wang and T. Zhang, *ChemSusChem*, 2010, **3**, 63–66.

17 Z. Tai, J. Zhang, A. Wang, M. Zheng and T. Zhang, *Chem. Commun.*, 2012, **48**, 7052–7054.

18 Y.-L. Cao, J.-W. Wang, Q.-F. Li, N. Yin, Z.-M. Liu, M.-Q. Kang and Y.-L. Zhu, *J. Fuel Chem. Technol.*, 2013, **41**, 943–949.

19 R. Geyer, J. Hunold, M. Keck, P. Kraak, A. Pachulski and R. Schödel, *Chem. Ing. Tech.*, 2012, **84**, 160–164.

20 A. E. Zagli, J. L. Falconer and C. A. Keenan, *J. Catal.*, 1979, **56**, 453–467.

21 C. Araujo-Andrade, F. Ruiz, J. R. Martínez-Mendoza and H. Terrones, *J. Mol. Struct. (THEOCHEM)*, 2005, **714**, 143–146.

22 K. K. Pandey and K. S. Theagarajan, *Holz als Roh- und Werkstoff*, 1997, **55**, 383–390.

23 J. Ibarra, E. Muñoz and R. Moliner, *Org. Geochem.*, 1996, **24**, 725–735.

24 B. M. Kabyemela, T. Adschiri, R. M. Malaluan and K. Arai, *Ind. Eng. Chem. Res.*, 1999, **38**, 2888–2895.

25 X. Sun and Y. Li, *Angew. Chem., Int. Ed.*, 2004, **43**, 597–601.

26 M. Sevilla and A. B. Fuertes, *Carbon*, 2009, **47**, 2281–2289.

27 M. Liebeck, C. Pfeifer, A. Drochner and G. H. Vogel, *Chem. Ing. Tech.*, 2013, **85**, 516–522.

28 K.-I. Seri, T. Sakaki, M. Shibata, Y. Inoue and H. Ishida, *Bioresour. Technol.*, 2002, **81**, 257–260.

29 Y. Roman-Leshkov, C. J. Barrett, Z. Y. Liu and J. A. Dumesic, *Nature*, 2007, **447**, 982–985.

30 J. Lewkowski, *ARKIVOC*, 2001, 17–54.

31 H. Yan, Y. Yang, D. Tong, X. Xiang and C. Hu, *Catal. Commun.*, 2009, **10**, 1558–1563.

32 H. Zhao, J. E. Holladay, H. Brown and Z. C. Zhang, *Science*, 2007, **316**, 1597–1600.

33 S. Lima, P. Neves, M. M. Antunes, M. Pillinger, N. Ignatyev and A. A. Valente, *Appl. Catal., A*, 2009, **363**, 93–99.

34 Q. Bao, K. Qiao, D. Tomida and C. Yokoyama, *Catal. Commun.*, 2008, **9**, 1383–1388.

35 Y. Su, H. M. Brown, X. Huang, X.-D. Zhou, J. E. Amonette and Z. C. Zhang, *Appl. Catal., A*, 2009, **361**, 117–122.

36 C. Li, Z. Zhang and Z. K. Zhao, *Tetrahedron Lett.*, 2009, **50**, 5403–5405.

37 R. Rinaldi, N. Meine, J. vom Stein, R. Palkovits and F. Schüth, *ChemSusChem*, 2010, **3**, 266–276.

38 L. Peng, L. Lin, J. Zhang, J. Zhuang, B. Zhang and Y. Gong, *Molecules*, 2010, **15**, 5258–5272.

39 A. Onda, T. Ochi and K. Yanagisawa, *Top. Catal.*, 2009, **52**, 801–807.

40 J. Pang, A. Wang, M. Zheng and T. Zhang, *Chem. Commun.*, 2010, **46**, 6935–6937.

41 A. Wang and T. Zhang, *Acc. Chem. Res.*, 2013, **46**, 1377.

42 A. Lackner, A. Filzwieser, P. Paschen and W. Köck, *Int. J. Refract. Met. Hard Mater.*, 1996, **14**, 383–391.

43 S. Kohl, Ph.D. Thesis, TU Darmstadt, 2010.

44 B. Kusserow, S. Schimpf and P. Claus, *Adv. Synth. Catal.*, 2003, **345**, 289–299.

45 S. Herdin, G. Kettenbach and P. Klüfers, *Z. Naturforsch., B: Chem. Sci.*, 2004, **59**, 134–139.

46 A. Kazemzadeha, A. Eskandaria and F. Goudarzia, Proc. 4th Int. Conf. Nanostructures (ICNS4), 12–14 March, 2012, Kish Island, I.R. Iran, 684–686.

47 E. Lassner and W. D. Schubert, in *Tungsten: Properties, Chemistry, Technology of the Element, Alloys, and Chemical Compounds*, Kluwer Academic/Plenum Publishers, New York, Boston, Dordrecht, London, Moscow, 1998.

48 Y. Liu, C. Luo and H. Liu, *Angew. Chem., Int. Ed.*, 2012, **51**, 3249–253.